ENGINEERING RESEARCH JOURNAL (ERJ)
Vol. 51, No. 4October. 2022, pp.239-248
Journal Homepage: https://erjsh.journals.ekb.eg/

Design and control Implementation of Adaptive Soft Gripper Installed on KUKA KR6 R900 Robot Arm

Shady A. Maged [1], Ehab M. Faidallah [2,3,*], Yehia H. Hossameldin [4], Saber Abd Raboo[2], Mahmoud Elsamanty [2, 5]

[1] Department of Mechatronics Engineering Department, Ain Shams University, Egypt

[2] Department of Mechanical Engineering Department, Benha University, Egypt

[3] Department of Mechatronics Engineering Department, The Higher Technological Institute, Egypt

[4] Department of Mechatronics Engineering Department, Future University, Egypt

[5] Mechatronics and Robotics Department, School of Innovative Design, Egypt-Japan University for Science and Technology, Egypt, Egypt

*Corresponding author

Abstract

For the last decades, industrial manipulator robots have been the best way for factories to automate their applications to save money and time with mass production. There are many applications the industrial robot can do like welding, assembly, packaging, and pick and place. So, the researcher head to improving and developing the end-effectors tools for wide application for industrial robots. This paper presents the full KUKA KR6 R900 kinematic with complete workspace analysis. Also designs and implements an adaptive soft gripper with a low-cost budget and lightweight as an end-effector tool. This gripper can grip various objects of various shapes, so it can save time instead of wasting time by replacing the grippers to fit the object or the product. The results show that the adaptive gripper can successfully grasp many objects of various shapes. Also, it can grasp gently without harming or damaging the object. Furthermore, the kinematics solution of the KUKA manipulator robot was presented. Finally, the complete workspace for the KUKA KR6 R900 was analyzed and presented.

Keywords: KUKA KR6 R900, Adaptive Gripper, Serial Manipulator, 6-DOF.

1. Introduction

It is well known that serial manipulator robots have numerous applications in various fields. In contrast, it can save time, reduce cost, and grant mass production because it is characterized by precision and speed. Different industrial applications for the serial manipulator robots are presented as a joints dynamic model was proposed for the universal robot UR5e to accurately predict the actuator torques required to realize the desired task [1]. Also, an object sorting robot manipulator

was developed by using a vision system to sort objects based on size, shape, and color [2]. In addition, for medical issues, these manipulators can achieve the required mission as in [3] they enhanced the precision and comfort of operation by proposing a physical human-robot interaction control scheme of the haptic master manipulator used in laparoscopic surgical robots, while avoiding errors in surgical instruments sorting tasks they improved a coordinate control strategy based on fuzzy hybrid control for dual arm coordinated operation [4]. Newley manipulators have been merged in the underwater application by mounting a robotic arm to a remotely operated underwater vehicle (ROV) for handling [5]. Moreover, the cartesian manipulator is used in agriculture to prune apple trees [6]. Lately, Manipulators have a place in aerospace as well by presenting a control of space robot manipulator (SRM) to capture a passive space vehicle (PSV) [7]. Because previous research has revealed numerous applications for the manipulator, it will require a variety of end-effectors to deal with the object and complete its mission perfectly and correctly.

A survey of different soft robotics gripper systems was presented and discussed [8]. A group of twelve objects with various mechanical and geometrical properties has been chosen for the laboratory experiments. They fabricated and tested four grippers. Two with pneumatic actuation, while the other two with electromechanical actuation. Moreover, they evaluated the environmental condition's effect on the grippers by evaluating each object in three different environments (normal, humid, and dusty). Finally, this provisional study aims to show the various performances of various grippers, which are evaluated under the same conditions. The results show that the mechanical gripper with a passive structure display greater robustness. A scheme was suggested to enhance the dexterous manipulation functionalities of two-fingered grippers to enhance the link dimension of the finger and interfinger distance for a specific object, as well as to identify how the finger manipulation workspace can be affected due to the finger symmetry and the separation between the finger bottom frames [9]. The workspace analysis results inspire the creation of a multi-modal, robotic adaptive gripper.

While a robotic hand with underactuated three-fingered was designed, a performance evaluation was proposed [10]. A single actuator controls the hand's radially symmetric, prismatically actuated fingers. The finger mechanism is composed of just one joint finger linked to the prismatic joint by a passive rotational joint perpendicular to the palm. The rotary joints allow the fingers to switch between spherical and cylindrical grasps passively, whereas the finger joint enables the fingers to roll around the grasped element. Using the YCB grasping benchmark, they evaluate how well this design performs compared to two other underactuated hand designs, a concentric gripper with cylindrical fingers, and other models. The results show that the three-finger prismatic hand works well compared to other methods, especially when installed with only one joint finger.

On the other hand, a free, affordable, robotic gripper with a three-finger device mechanism was presented [11]. Following a detailed description of an underactuated finger, gear train structure, and a complete gripper assembly design. Also, there is a discussion of the gripper's grasping efficiency and potential gripper platform improvements. The gripper mechanism model was implemented with the help of an inexpensive servo motor and a small number of 3D-printed parts. The results show that the gripper cost is about 20% compared to a similar gripper. Also, the grippers succeed in grasping different objects correctly.

Moreover, [12] presents a robotic adaptive gripper composed of three-finger with an open-loop grasping methodology. They prove the robot's functionality and capabilities by conducting several grasping experiments. Then, various degrees of object stiffness were selected to demonstrate the grasping capability. The research results demonstrate a strong correlation between finger position, motor current, and force sensor, and the outcomes can also be applied to ensure adequate grasping effectiveness.

Furthermore, A novel hyper-adaptive robot hand that can distinguish between various common objects with only one grasp was demonstrated. [13]. The advantages of straightforward, adaptive grasping systems are fully utilized in this work. The feature space comprises the motor positions, contact forces, and Google Soli readings collected at various points during the grasping process. Experimental paradigms using models and common objects have been used to experimentally validate the effectiveness of the designs, sensors, and methodologies.

This work aims to design an under actuated adaptive soft gripper. This design will help the KUKA KR6 R900 to pick and place different objects of different shapes without wasting time replacing the grippers or damaging the objects. Then, to identify the end-effector's final orientation and position, a complete kinematic solution was presented in section 2. Moreover, the simulation and complete workspace analysis were analyzed

and presented in section 3. Furthermore, the laboratory test for the adaptive gripper was presented and discussed in section 4. Finally, the conclusions and results for the adaptive gripper are illustrated in section 5.

2. MATERIALS AND METHODS

The serial manipulator KUKA KR6 R900 has six revolute joints (O1, O2, O3, O4, O5, and O6) as shown in Fig. 1. The first three joints O1, O2, and O3 with motion range ±170°, -190°/45° and -120°/156° respectively can specify the position of manipulator end-effector position while the last three joints (O4, O5, and O6) with motion range ±185°, ±120°, and ±350° respectively can identify the manipulator end-effector orientation. The average payload for this manipulator is 3Kg, while 6 kg is the extreme payload. Moreover, the complete weight of the robotic manipulator is 52 kg.

FIGURE 1. Arbitrary Posture for KUKA RR6 R900

2.1 Direct Kinematic

The forward or direct kinematics is to identify the manipulator end-effector orientation and position with known joints angle (θ_i). The KUKA KR6 R900 has six joints angle (θ_1, θ_2, θ_3, θ_4, θ_5 and θ_6) where θ_1 guiding link O_0 O_1 , θ_2 guiding link O_1 O_2 , θ_3 guiding link O_2 O_3 , θ_4 guiding link O_3 O_4 , θ_5 guiding link O_4 O_5 while θ_6 for link O_5 O_6 as illustrated in Fig 2.

A 4x4 matric will describe each joint in the frame system, where (R) represents the orientation of the end-effector and (T) denote the end-effector position, as shown in the following form:

$$A_i^{i-1} = \begin{bmatrix} R & R & R & T \\ R & R & R & T \\ R & R & R & T \\ 0 & 0 & 0 & 1 \end{bmatrix}$$

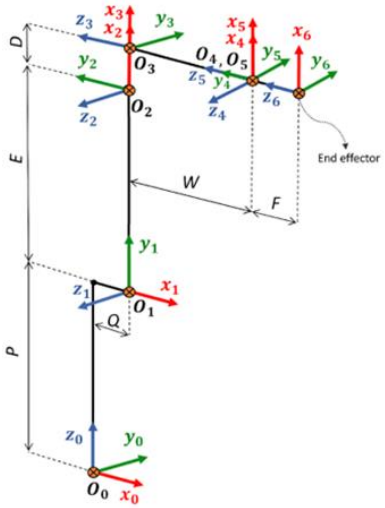

FIGURE 2. KUKA KR6 R900 Kinematic Model

By applying Denavit-Hatenburg (D-H) method see Table 1, the transformation matrix between O_0 and O_6 a can be obtained using the general matrix form [14]:

TABLE 1: KUKA KR6 R900 D-H parameters

Link i	α_i (degree)	a_i (mm)	d_i (mm)	θ_i (degree)
0-1	-90	Q	P	θ_1
1-2	0	E	0	$\theta_2 - 90$
2-3	90	D	0	θ_3
3-4	-90	0	-W	θ_4
4-5	-90	0	0	θ_5
5-6	0	0	F	θ_6

Finally, T_6^0 can be obtained by multiplying matrices $T_1^0, T_2^1, T_3^2, T_4^3, T_5^4$, and T_6^5 as in equation (1).

$$T_6^0 = T_1^0 . T_2^1 . T_3^2 . T_4^3 . T_5^4 . T_6^5 = \begin{bmatrix} n_x & o_x & a_x & p_x \\ n_y & o_y & a_y & p_y \\ n_z & o_z & a_z & p_z \\ 0 & 0 & 0 & 1 \end{bmatrix} \quad (1)$$

Where, $\begin{bmatrix} n_x & o_x & a_x \\ n_y & o_y & a_y \\ n_z & o_z & a_z \end{bmatrix}$ presents the end-effector orientation while $\begin{bmatrix} p_x \\ p_y \\ p_z \end{bmatrix}$ Presents the position as illustrated in equations from (2) to (13) the solution of the final matrix parameters.

Note that to simplify writing equations C represent cos and S represent sin also

$C_{1,2,n} = \cos(\theta_1)\cos(\theta_2)\cos(\theta_n)$ or

$S_{1,2,n} = \sin(\theta_1)\sin(\theta_2)\sin(\theta_n)$.

$$\boldsymbol{n_x} = C_4S_{1,6} - C_5S_{1,4} + C_{1,2,3}S_{4,6} - C_{1,2,6}S_{3,5} - C_{1,3,6}S_{2,5} - C_1S_{2,3,4,6} + C_{1,2,3,4,5,6} - C_{1,4,5,6}S_{23} \quad (2)$$

$$\boldsymbol{n_y} = C_{1,5,6}S_4 - C_{1,4}S_6 + C_{2,3}S_{1,4,6} - C_{2,6}S_{1,3,5} - C_{3,6}S_{1,2,5} - S_{1,2,3,4,6} + C_{2,3,4,5,6}S_1 - C_{4,5,6}. \quad (3)$$

$$\boldsymbol{n_z} = C_6S_{2,3,5} - C_2S_{3,4,6} - C_3S_{2,4,6} - C_{2,3,6}S_5 - C_{2,4,5,6}S_3 - C_{3,4,5,6}S_2 \quad (4)$$

$$\boldsymbol{o_x} = C_{4,6}S_1 + C_5S_{1,4,6} + C_{1,2,3,6}S_4 - C_{1,6}S_{2,3,4} + C_{1,2}S_{3,5,6} + C_{1,3}S_{2,5,6} - C_{1,2,3,4,5,6} + C_{1,4,5}S_{2,3,6} \quad (5)$$

$$\boldsymbol{o_y} = C_{2,3,6}S_{1,4} - C_{1,5}S_{4,6} - C_{1,4,6} - C_6S_{1,2,3,4} + C_2S_{1,3,5,6} + C_3S_{1,2,5,6} - C_{2,3,4,5}S_{1,6} + C_{4,5}S_{1,2,3,6} \quad (6)$$

$$\boldsymbol{o_z} = C_{2,3}S_{5,6} - C_{3,6}S_{2,4} + C_{2,6}S_{3,4} - S_{2,3,5,6} + C_{2,4,5}S_{3,6} + C_{3,4,5}S_{2,6} \quad (7)$$

$$\boldsymbol{a_x} = S_{1,4,5} - C_{1,2,5}S_3 - C_{1,3,5}S_2 - C_{1,2,3,4}S_5 + C_{1,4}S_{2,3,5} \quad (8)$$

$$\boldsymbol{a_y} = C_4S_{1,2,3,5} - C_{2,5}S_{1,3} - C_{3,5}S_{1,2} - C_{2,3,4}S_{1,5} - C_1S_{4,5} \quad (9)$$

$$\boldsymbol{a_z} = C_5S_{2,3} - C_{2,3,5} + C_{2,4}S_{3,5} + C_{3,4}S_{2,5} \quad (10)$$

$$\boldsymbol{p_x} = QC_1 + EC_{1,2} + DC_{1,2,3} - DC_1S_{2,3} + WC_{1,2}S_3 + WC_{1,3}S_2 + FS_{1,4,5} - FC_{1,2,5}S_3 - FC_{1,3,5}S_2 + FC_{1,4}S_{2,3,5} - FC_{1,2,3,4}S_5 \quad (11)$$

$$\boldsymbol{p_y} = QS_1 + EC_2S_1 + DC_{2,3}S_1 + FC_1S_{4,5} - DS_{1,2,3} + WC_2S_{1,3} + WC_3S_{1,2} - FC_{2,5}S_{1,3} - FC_{3,5}S_{1,2} + FC_4S_{1,2,3,5} - FC_{2,3,4}S_{1,5} \quad (12)$$

$$\boldsymbol{p_z} = P - ES_2 - DC_2S_3 - DC_3S_3 - DC_3S_2 + WC_{2,3} - WS_{2,3} - FC_{2,3,5} + FC_5S_{2,3} + FC_{2,4}S_{3,5} + FC_{3,4}S_{2,5} \quad (13)$$

2.2 Inverse Kinematic

The inverse kinematics is to determine the robot arm joints angle for the desired position (x_c,y_c,z_c) and orientation (A, B, C). Moreover, the inverse kinematic for the manipulator with six joints and a spherical wrist can be split into two problems (decoupling method); the first problem is solving inverse position, and the second problem is solving inverse orientation. So, by knowing the required position and orientation, the inverse solution for the first three joints, which are responsible for the position, can be solved graphically by using position data, while the last three joints can be solved with the analytical method with the help of Euler angles by using required orientation data [15].

$$\boldsymbol{\theta_1}: \tan\theta_1 = \frac{y_c}{x_c},\ \theta_1 = \text{atan2}(y_c, x_c) \quad (14)$$

$$\boldsymbol{\theta_2} = atan2\left(z_c - d_1, \sqrt{x_c^2 + y_c^2}\right) \pm atan2(l_2 sin\theta_3, l_1 + l_2 cos\theta_3) \quad (15)$$

$$\boldsymbol{\theta_3} = atan2\left(\sqrt{1 - D^2},\ D\right) \quad (16)$$

$$\boldsymbol{\theta_4} = atan2((c_{123} - c_1s_{23})r_{13} + (c_{23}s_1 - s_{123})r_{23} + (c_2s_3 + c_3s_2)r_{33}, -s_1r_{13} + s_1r_{23}) \quad (17)$$

$$\boldsymbol{\theta_5} = atan2((-c_{12}s_3 - c_{13}s_2)r_{13} - (c_2s_{13} + c_3s_{12})r_{23} + (c_{23} - s_{23})r_{33}, \pm \sqrt{1 - ((-c_{12}s_3 - c_{13}s_2)r_{13} - (c_2s_{13} + c_3s_{12})r_{23} + (c_{23} - s_{23})r_{33})^2} \quad (18)$$

$$\boldsymbol{\theta_6} = atan2(-c_{12}s_3 - c_{13}s_2)r_{11} - (c_2s_{13} + c_3s_{12})r_{21} + (c_{23} - s_{23})r_{31}, (-c_{12}s_3 - c_{13}s_2)r_{12} - (c_2s_{13} + c_3s_{12})r_{22} + (c_{23} - s_{23})r_{32} \quad (19)$$

3. KUKA KR6 R900 WORKSPACE AND RANGE LIMITATION

A graphical model for the KUKA KR6 R900 was provided by importing the CAD file into the MATLAB-SIMSCAPE platform, as shown in Fig. 3, to obtain the workspace for the manipulator robot. This simulation program is based on a Monte-Carlo method by providing the joints angle ($\theta_1, \theta_2, \theta_3, \theta_4, \theta_5$ and θ_6) as input and record the output position and orientation (x_c, y_c, z_c, A, B, C) for the end-effector. These recorded points will compose a sphere representing the KUKA arm robot workspace, as illustrated in Fig. 4.

FIGURE 3. KUKA KR6 R900 CAD Model to MATLAB-SIMSCAPE Platform

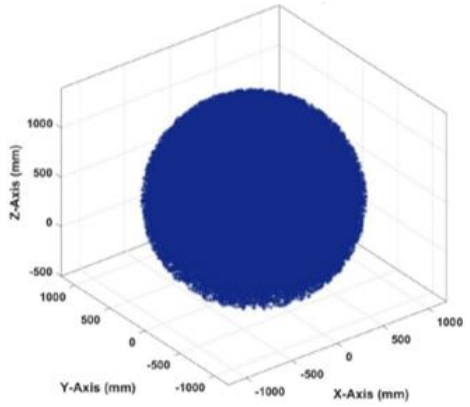

FIGURE 4. KUKA KR6 R900 3D Workspace

The KUKA KR6 R900 workspace was analyzed and discussed to identify the movement range limitations of the manipulator robot. The workspace was presented in two different planes (X-Z plane and Y-Z plane). As shown in Fig. 5(a) the 3D workspace with a side slice at X=0 to extract the 2D workspace for the robot in side-view (X-Z plane) as shown in fig. 5(b). While Fig. 5(c) displays the workspace-covered area. Moreover, Fig. 5(d) shows the motion range for side view (X-Z plane) with Xmax= 981.2 mm and Xmin = -931.2 mm while Zmax = 1356 mm and Zmin = -422.9 mm.

On the other side, Fig. 6(a) illustrates the 3D workspace with a front slice at Y=0 to extract the 2D workspace for the robot in front view (Y-Z plane), as shown in Fig. 6(b). while Fig. 6(c) displayed the workspace-covered area. Moreover, Fig. 6(d) shows the motion range for side view (Y-Z plane) with Ymax = 981.2 mm and Ymin = -981.2 mm while Zmax = 1356 mm and Zmin= -422.9 mm.

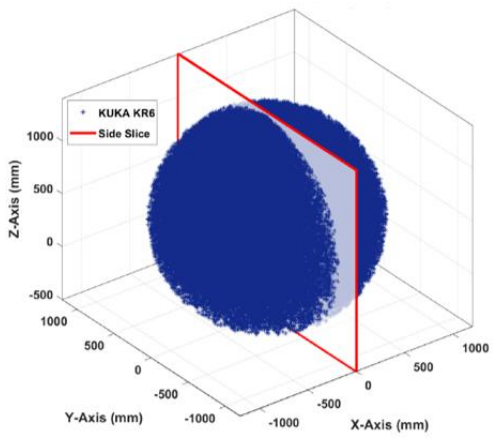

(a) KUKA KR6 R900 3D Workspace with Side View

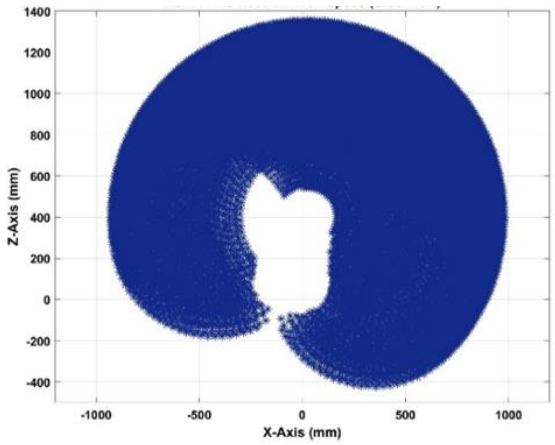

(b) KUKA KR6 R900 2D Workspace (Side View)

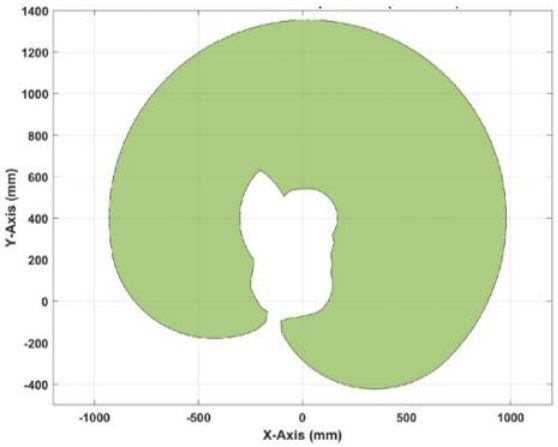

(c) KUKA KR6 R900 Area (Side View)

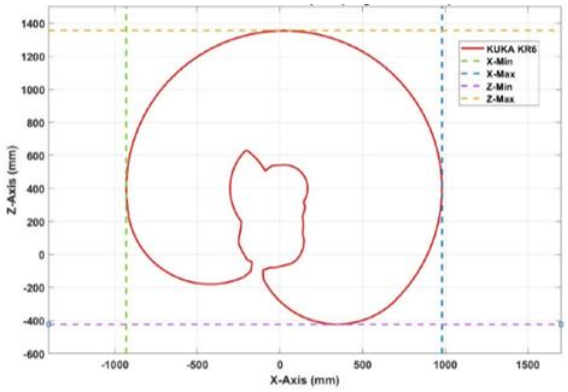

(d) KUKA KR6 R900 2D Workspace Motion Limitation and Range for Side View

FIGURE 5. KUKA KR6 R900 Workspace (Side View)

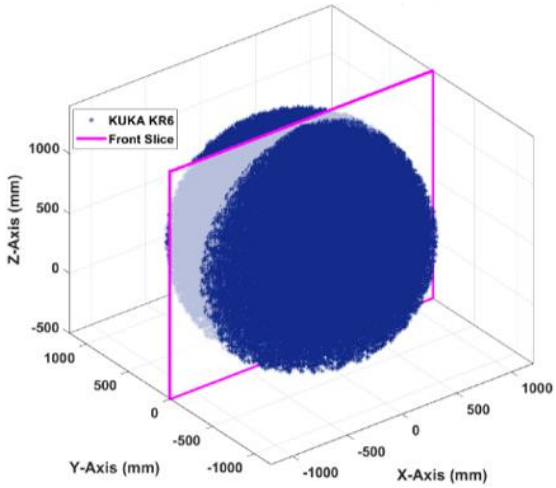

(a) KUKA KR6 R900 3D Workspace with Front View

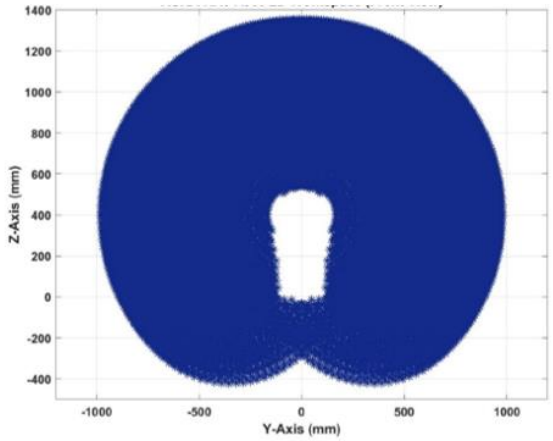

(b) KUKA KR6 R900 2D Workspace (Front View)

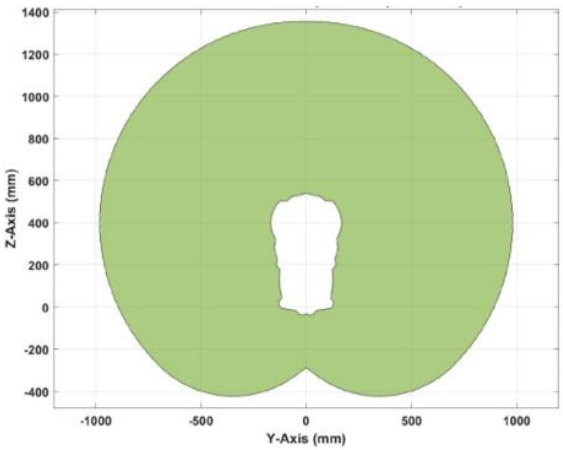

(c) KUKA KR6 R900 Area (Front View)

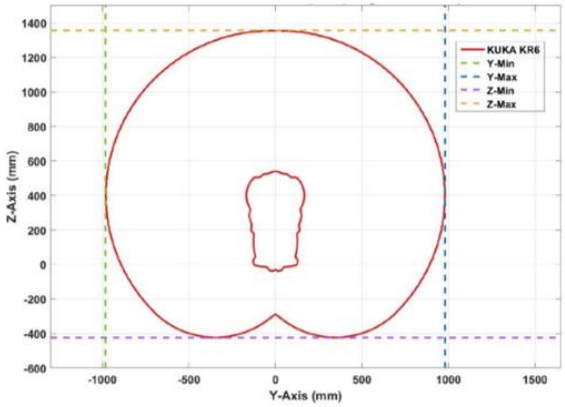

(d) KUKA KR6 R900 2D Workspace Motion Limitation and Range for Front View

FIGURE 6. KUKA KR6 R900 Workspace (Front View)

4. KUKA KR6 R900 WITH ADAPTIVE SOFT GRIPPER

The KUKA KR6 R900 is used in many industrial applications, and the common wide application is picking and placing. At the same time, the pick and place are used with different products with different shapes, so we will need to replace them with suitable grippers for each process. So, designing and implementing an adaptive gripper will solve this problem by grasping other objects of different shapes with the same gripper. Also, it will save more time in replacing grippers.

4.1. Adaptive Soft Gripper Design

The adaptive gripper is designed with a low-cost budget and is lightweight compared to [11] which presented a low-cost adaptive gripper with a budget 327.92$ while our design cost about 58.89$ as shown in table 2 which means that the new proposed design will save about 82% in budget with providing sufficient efficiency and performance for the grasping process. Also, they mentioned that the gripper weight is about 500 grams while our actual gripper weight is about 186 grams which means the new design presents more lightweight by 62.8% than the other design. This gripper design was inspired by the human hand but with only three fingers, and the angle between each finger is 120°, as in Fig. 7(b). Each finger contains three tips, while the upper tip, middle tip, and lower tip in the adaptive gripper finger represent the distal phalange (DP), intermediate phalange (IP), and proximal phalange (PP) in the human hand finger,

respectively as shown in Fig. 7(c). the finger was supported with a flat slice of rubber which helps to connect the three tips as in Fig. 8. For flexible finger bending, a chamfer on both sides of the tip was considered with the distribution of the tips in equal spaces along the rubber. this design will permit the finger to bend like the joints of the human finger (Metacarpal Interphalangeal Joint, Proximal Interphalangeal Joint, and Distal Interphalangeal Joint).

TABLE 2: Adaptive Gripper Total Cost

Item	Source	Quantity	Total cost
Spacer 5cm	RAM Shop	3	0.25$
Spacer 1.5cm	RAM Shop	3	0.25$
Spacer 0.5cm	RAM Shop	3	0.25$
Screw 3mm	RAM Shop	6	0.5$
M2 screw (motor)	Robotis	4	free
Base	3D-Printed	2	1.9$
Motor holder	3D-Printed	1	1.56$
Gripper holder	3D-Printed	1	1.38$
Wire pully	3D-Printed	1	0.7$
DYNAMIXEL AX12	Robotis	1	49$
Rubber (Flat slice)	Rubber shop	3	1$
DP Base & Cap	3D-Printed	3	0.5$
IP Base & Cap	3D-Printed	3	1$
PP Base & Cap	3D-Printed	3	0.6$
		Overall	58.89$

(a) Isometric View

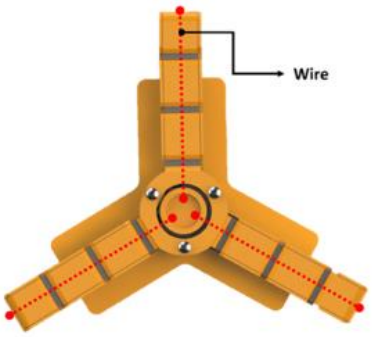

(b) Front View

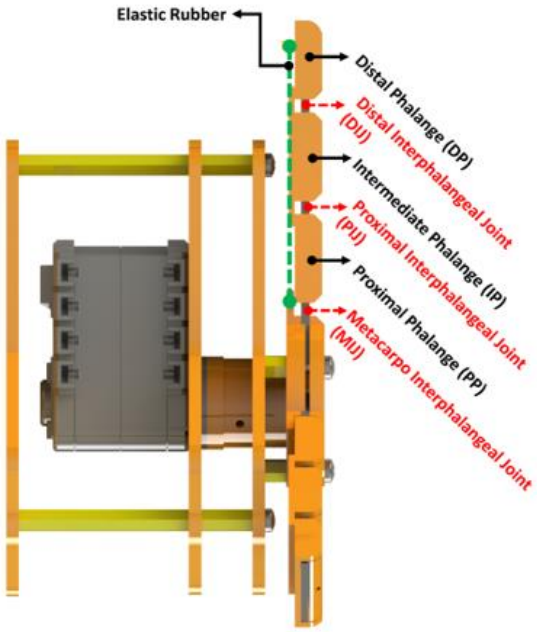

(c) **(c)** Side View

FIGURE 7. Adaptive Gripper

The operation concept depends on three underactuated fingers with a pully driven by a servo motor, as shown in Fig. 8. When the motor moves in the CW direction, it will make the fingers bent under the effect of a nylon wire fixed through each finger as in Fig. 7(b), and when the motor moves in CCW direction, the elastic rubber as shown in Fig. 7(c) will return the finger back to its initial position.

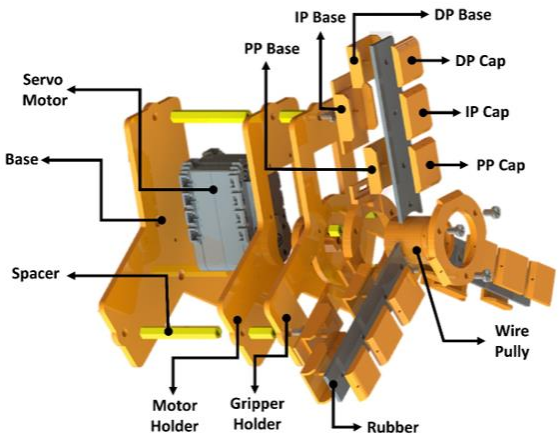

FIGURE 8. Adaptive Gripper (Exploded View)

4.2. KUKA KR6 R900 With Adaptive Soft Gripper

The adaptive gripper was attached with the KUKA KR6 R900 flange using three 5mm screws as shown in Fig. 9, while Fig. 10 illustrates a posture for the proposed and real models. After mounting the adaptive gripper with the help of the inverse kinematics solution to identify the required

angle to reach the required position and workspace analysis to identify the robot range limitation, the robotic arm is ready to pick and place any objects from one point to another, as shown in Fig. 11.

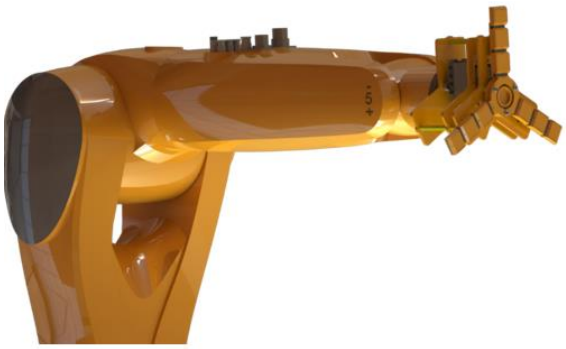

FIGURE 9. KUKA KR6 R900 with Adaptive Gripper (CAD Model)

(a) CAD Model **(b)** Real Model

FIGURE 10. Posture for KUKA KR6 R900 with Adaptive Gripper

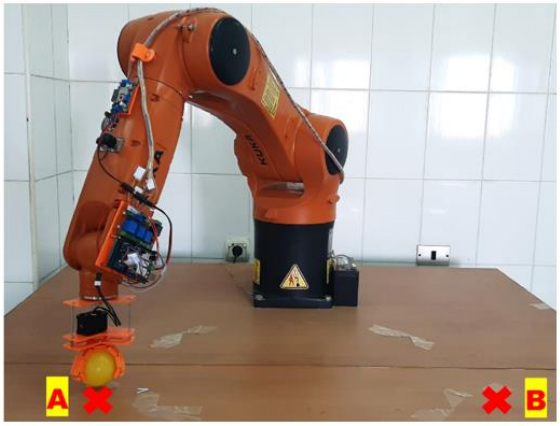

FIGURE 11. Pick and Place operation using Adaptive Gripper

4.3. Adaptive Gripper Testing

A laboratory test for the adaptive gripper was done using ten different objects of various shapes. The result indicates that the adaptive gripper succeeded in grasping most objects such as ball (sphere shape), carton box (square shape), water bottle (cylindrical shape), lamp, cup (partial cone), whiteboard eraser (rectangular shape), roller tape and remote control as shown in Fig.12(a), Fig.12(b), Fig.12(c), Fig.12(d), Fig.12(e), Fig.12(f), Fig.12(g) and Fig.12(h) respectively, while the gripper failed to grasp the object with small geometrical shapes like pen or coin as shown in table 3.

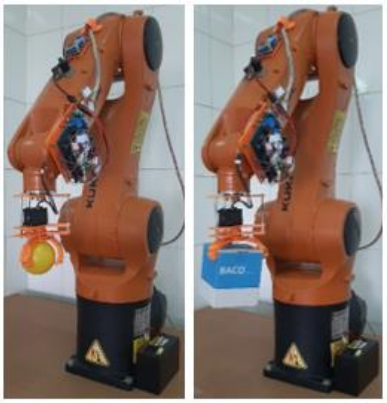

(c) (d)

(e) (f)

(g) (h)

FIGURE 12. Adaptive Gripper Laboratory Test

TABLE 3: Grasping Objects Trials

	Object	Trial Result
1	**Ball**	Pass
2	**Carton box**	Pass
3	**Water bottle**	Pass
4	**Lamp**	Pass
5	**Cup**	Pass
6	**Whiteboard eraser**	Pass
7	**Roller tape**	Pass
8	**Remote control**	Pass
9	**Pen**	Failed
10	**Coin**	Failed

5. CONCLUSIONS AND OUTCOMES

An adaptive soft gripper was designed and implemented to grasp different objects of various shapes with taking into consideration the aspect limitation of the gripper. This gripper design is characterized by a low-cost and lightweight also the mechanism allows the finger to bend with a sufficient angle to grasp the object tightly and gently without destroying or damaging the object. The proposed mechanism is represented in a CAD model. Also, a complete workspace analysis for the KUKA manipulator robot was introduced to identify the robot's motion range limitation. Finally, a laboratory test was implemented, and the results show that the adaptive gripper succeeded in grasping eight different objects of different shapes without any damage while it failed to grasp objects with small geometrical shapes such as coins and pens. So, it recommends enhancing the finger's tip design to improve gripper grasping and also adding a force sensor on the finger of the gripper to control grasping force not only depending on the mechanical design in grasping.

6. REFERENCES

[1] E. Madsen, O. S. Rosenlund, D. Brandt, and X. Zhang, "Comprehensive modeling and identification of nonlinear joint dynamics for collaborative industrial robot manipulators," *Control Eng. Pract.*, vol. 101, no. January, p. 104462, 2020, doi: 10.1016/j.conengprac.2020.104462.

[2] M. H. Ali, K. Aizat, K. Yerkhan, T. Zhandos, and O. Anuar, "Vision-based Robot Manipulator for Industrial Applications," *Procedia Comput. Sci.*, vol. 133, pp. 205–212, 2018, doi: 10.1016/j.procs.2018.07.025.

[3] Z. Du, Y. Liang, Z. Yan, L. Sun, and W. Chen, "Human-robot interaction control of a haptic master manipulator used in laparoscopic minimally invasive surgical robot system," *Mech. Mach. Theory*, vol. 156, p. 104132, 2021, doi: 10.1016/j.mechmachtheory.2020.104132.

[4] Q. Wu, M. Li, X. Qi, Y. Hu, B. Li, and J. Zhang, "Coordinated control of a dual-arm robot for surgical instrument sorting tasks," *Rob. Auton. Syst.*, vol. 112, pp. 1–12, 2019, doi: 10.1016/j.robot.2018.10.007.

[5] S. Hachicha, C. Zaoui, H. Dallagi, S. Nejim, and A. Maalej, "Innovative design of an underwater cleaning robot with a two arm manipulator for hull cleaning," *Ocean Eng.*, vol. 181, no. April 2018, pp. 303–313, 2019, doi: 10.1016/j.oceaneng.2019.03.044.

[6] A. Zahid, M. S. Mahmud, L. He, D. Choi, P. Heinemann, and J. Schupp, "Development of an integrated 3R end-effector with a cartesian manipulator for pruning apple trees," *Comput. Electron. Agric.*, vol. 179, no. August, p. 105837, 2020, doi: 10.1016/j.compag.2020.105837.

[7] Y. Somov, S. Butyrin, and S. Somov, "Guidance and control of a space robot-manipulator at approach and capturing a passive satellite," *IFAC-PapersOnLine*, vol. 52, no. 12, pp. 538–543, 2019, doi: 10.1016/j.ifacol.2019.11.299.

[8] S. Terrile, M. Argüelles, and A. Barrientos, "Comparison of different technologies for soft robotics grippers," *Sensors*, vol. 21, no. 9, 2021, doi: 10.3390/s21093253.

[9] N. Elangovan, L. Gerez, G. Gao, and M. Liarokapis, "Improving Robotic Manipulation without Sacrificing Grasping Efficiency: A Multi-Modal, Adaptive Gripper with Reconfigurable Finger Bases," *IEEE Access*, vol. 9, pp. 83298–83308, 2021, doi: 10.1109/ACCESS.2021.3086802.

[10] S. B. Backus and A. M. Dollar, "An Adaptive Three-Fingered Prismatic Gripper with Passive Rotational Joints," *IEEE Robot. Autom. Lett.*, vol. 1, no. 2, pp. 668–675, 2016, doi: 10.1109/LRA.2016.2516506.

[11] K. Telegenov, Y. Tlegenov, and A. Shintemirov, "A low-cost open-source 3-D-printed three-finger gripper platform for research and educational purposes," *IEEE Access*, vol. 3, pp. 638–647, 2015, doi: 10.1109/ACCESS.2015.2433937.

[12] A. S. Sadun, J. Jalani, and F. Jamil, "Grasping analysis for a 3-Finger Adaptive Robot Gripper," *2016 2nd IEEE Int. Symp. Robot. Manuf. Autom. ROMA 2016*, no. 3, 2017, doi: 10.1109/ROMA.2016.7847806.

[13] Z. Flintoff, B. Johnston, and M. Liarokapis, "Single - Grasp , Model - Free Object Classification using a Hyper - Adaptive Hand , Google Soli , and Tactile Sensors"2018 IEEE/RSJ International Conference on Intelligent Robots and Systems (IROS). 1943–1950. https://doi.org/10.1109/IROS. 2018.8594166.

[14] L. Tsai, "Robot analysis: the mechanics of serial and parallel manipulators," *The Mechanics of Serial and Parallel Manipulators*. p. 520, 1999.

[15] M. W. Spong, S. Hutchinson, and M. Vidyasagar, "Robot modeling and control," *IEEE Control Syst.*, vol. 26, no. 6, pp. 113–115, 2006, doi: 10.1109/MCS.2006.252815.